A Letters Journal Exploring the Frontiers of Physics

August 2008

EPL, **83** (2008) 47003
doi: 10.1209/0295-5075/83/47003

www.epljournal.org

Observation of an inverted band structure near the surface of InN

L. Colakerol[1], L. F. J. Piper[1], A. Fedorov[2], T. C. Chen[3], T. D. Moustakas[3] and K. E. Smith[1(a)]

[1] *Department of Physics, Boston University - Boston, MA 02215, USA*
[2] *Advanced Light Source, Lawrence Berkeley National Laboratory - Berkeley, CA, USA*
[3] *Department of Electrical and Computer Engineering, Boston University - Boston, MA 02215, USA*

received 30 April 2008; accepted 23 June 2008
published online 29 July 2008

PACS 79.60.Bm – Clean metal, semiconductor, and insulator surfaces
PACS 73.20.At – Surface states, band structure, electron density of states
PACS 71.20.Nr – Semiconductor compounds

Abstract – The dispersion of the valence band within the electron accumulation layer of n-type InN$(000\bar{1})$ has been directly measured using angle-resolved photoemission spectroscopy. Intermixing between the heavy-hole and light-hole valence bands in the intrinsic quantum well potential associated with the near-surface electron accumulation layer results in an inverted band structure, with the valence band maximum lying away from the Brillouin zone center. Such an inverted band structure has not previously been observed in an intrinsic accumulation layer.

Electrons in the accumulation layer near the surface of InN have recently been discovered to exist in intrinsic quantum well states [1]. The confining quantum well potential is perpendicular to the sample surface, and is formed by downward band bending when the Fermi level (E_{F}) is pinned high above the conduction band minimum near the surface of InN [2]. The fact that the quantum well exists near the surface allows angle-resolved photoemission spectroscopy (ARPES) to be used to study the detailed electronic structure of states within this semiconductor quantum well [1]. This is highly advantageous, since ARPES cannot in general be used to study the electronic structure of conventional engineered semiconductor quantum wells as these are usually buried well below the sample surface. ARPES can, of course, be used to study the electronic structure of quantum wells grown on surfaces, such as those formed by metal overlayers [3]. However, the existence of a quantum well potential near the surface of InN allows ARPES to probe the behavior of intrinsic, bulk InN states in the presence of such a potential for the first time.

We report here the results of an ARPES study of the dispersion of valence band states of InN$(000\bar{1})$ within the confining near-surface potential well. A *minimum* in the dispersion of the top of the valence band is measured at the zone center (Γ-point) in the presence of the quantized electron sub-bands in the conduction band. InN is well known to be a direct gap semiconductor in the bulk, and our measurement of a zone center minimum for the energy of the valence band maximum (VBM), is ascribed to mixing between the heavy- and light-hole valence bands within the electron accumulation layer. This phenomenon is known as an inverted band structure, and has been reported in transport and tunneling experiments from single HgTe/$\mathrm{Hg}_{1-x}\mathrm{Cd}_x\mathrm{Te}$ [4] and GaAs/AlAs quantum wells [5]. An inverted band structure has also been measured in an ARPES study of an *extrinsic* quantum well formed by an indium overlayer on p-type Si(111) [6]. However, the fact that the existence of an electron accumulation layer and confining potential can result in an inverted band structure near the surface of a clean semiconductor has not been reported before.

The experiments were undertaken on beamline 12.0.1 at the Advanced Light Source (ALS), Lawrence Berkeley National Laboratory. This beamline is equipped with 100 mm hemispherical electron energy analyzer (Scienta SES100). Typical energy and full angular resolution were 35 meV and 0.5°. The InN films were grown on c-plane sapphire substrates by radio frequency plasma-assisted molecular beam epitaxy [7]. The films were auto-doped n-type with an average carrier concentration of $5 \times 10^{19}\,\mathrm{cm}^{-3}$ and an average electron mobility of $340\,\mathrm{cm}^2/\mathrm{V}\cdot\mathrm{s}$. The room temperature optical gap was approximately 0.77 eV as determined by the peak of the derivative of the absorption constant. This is consistent with a fundamental energy band gap of 0.65 eV [8,9]; *i.e.* there is a Moss-Burstein shift of the optical absorption to higher energy due to degenerate doping [8]. Samples

(a) E-mail: ksmith@bu.edu

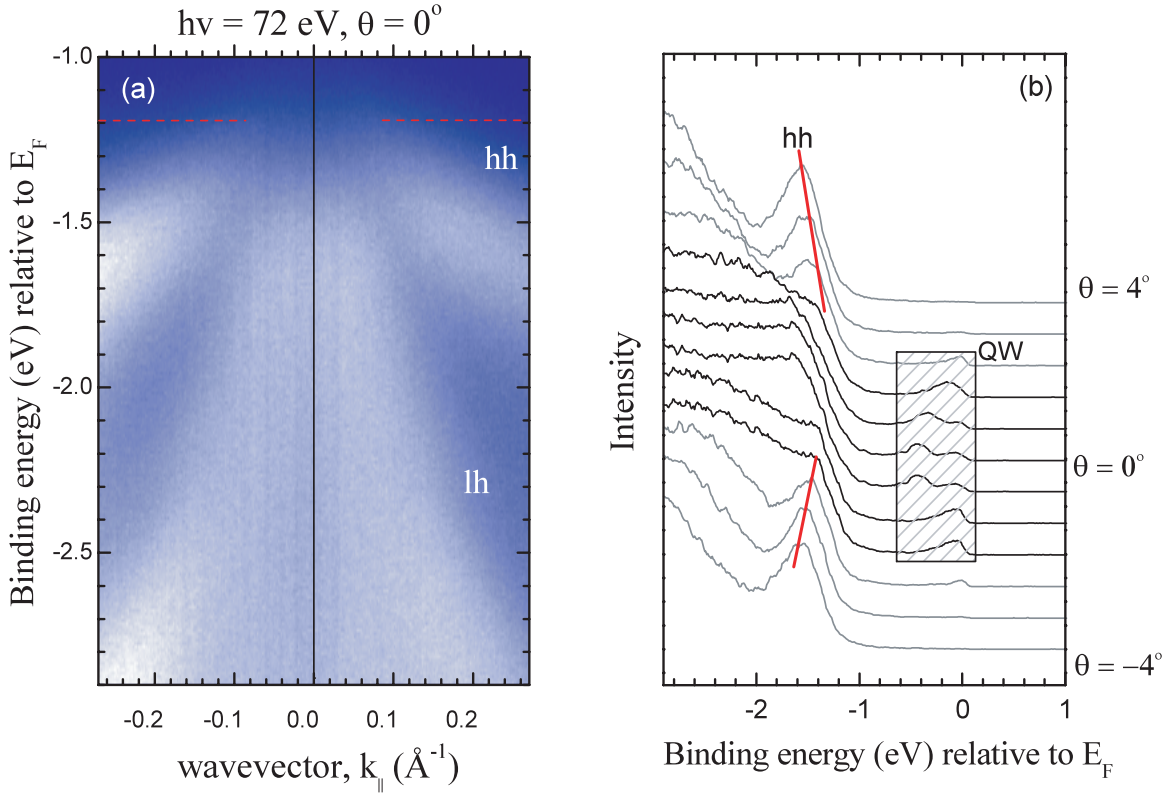

Fig. 1: (a) ARPES photocurrent intensity map of the valance band dispersion of InN. (b) The corresponding EDC spectra, with an enlarged binding energy axis. The quantum well (QW) states are clearly identified. The spectra within this region have been highlighted. Guides to the eyes have been added to display the valence band dispersion of the topmost bands.

were cleaned by low-temperature annealing ($\sim 400\,^{\circ}$C) in ultra-high vacuum (UHV), base pressure typically $< 1 \times 10^{-10}$ torr. All surfaces exhibited sharp (1×1) low-energy electron diffraction (LEED) patterns with a low background at an incident electron energy of 37 eV. ARPES spectra were recorded with the sample temperature at 60 K.

Figure 1(a) presents the ARPES photocurrent intensity map from the top of the valence band. The ARPES intensity map was recorded with the sample normal to the detector and with an incident photon energy of 72 eV. The horizontal axis is the angle of emission, converted to wave vector parallel to the surface ($k_{\|}$) at each point; the momentum direction is parallel to the ΓΣM line in the bulk Brillouin zone. The vertical axis is the binding energy with respect to the pinned Fermi level (zero binding energy). The intensity reflects the photocurrent for any particular binding energy and $k_{\|}$. Two dispersing bands, symmetric around the surface zone center ($k_{\|} = 0\,\text{Å}^{-1}$), are clearly visible. These correspond conventionally to the heavy-hole and light-hole valence bands. It is immediately clear that the intensity of the heavy-hole valence band vanishes near the zone center, resulting in a camel-back dispersion of the top of the valence band. This also visible in fig. 1(b), which plots the energy dispersion curves (EDCs) extracted from the data in fig. 1(a). Whereas the intensity map of fig. 1(a) focuses on the states at the top of the valence band, the EDCs in fig. 1(b) include the quantum well states at E_{F}. Two quantum well states are visible, and these have been discussed at length elsewhere [1]. They disperse symmetrically around $0\,\text{Å}^{-1}$, with an angular spread of $\pm 2°$ for $h\nu = 72$ eV; the subband minima lie at -450 meV and -200 meV below E_{F}. The spectral peak associated with the heavy-hole band is marked in fig. 1(b), and this peak is suppressed in exactly the range of angles where the quantum well states are visible.

Figure 2 displays a photocurrent intensity map for states near the top of the valence band at a binding energy of 1.35 eV below E_{F}. This was recorded using an incident photon energy of 72 eV. This plot shows the two-dimensional extent in momentum space of the minimum near the top of the valence band around the surface zone center. As is clear in fig. 2, the valence band maximum lies 0.15–0.20 Å^{-1} from Γ in all directions, which corresponds to the limit of the influence of the QW states as displayed in fig. 1.

There is a significant body of experimental evidence that InN is a direct gap semiconductor, including a recent study of the bulk electronic structure using resonant X-ray emission spectroscopy and state-of-the-art hybrid density functional theory [10]. The origin of the zone center

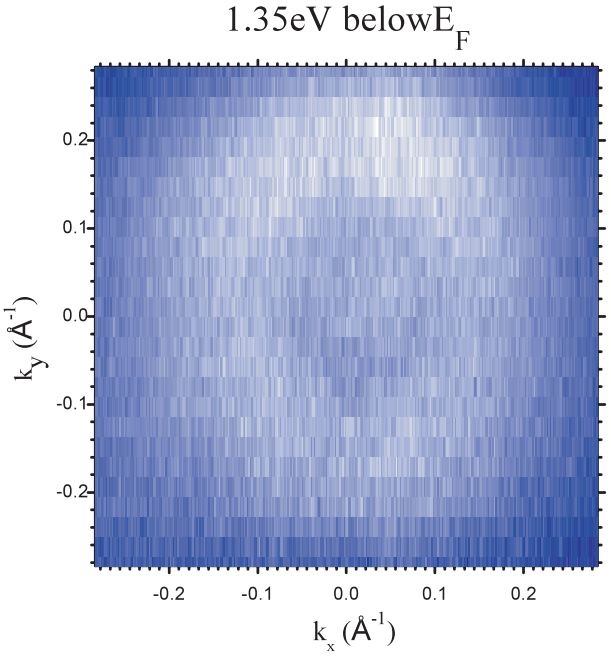

Fig. 2: Measured valence band constant energy contour at 1.5 eV below E_{F}.

minimum in the VBM observed in the present ARPES study must thus be related to the surface sensitivity of the spectroscopy. In short, given that the electron accumulation layer extends up to 80 Å into the bulk from the semiconductor-vacuum interface [2,11], ARPES measurements reflect the valence band in the presence of this accumulation layer, and associated confining potential. The minimum observed for the VBM at the zone center can then be understood as the result of the quantum well potential causing an intermixing between the light- and heavy-hole bands, resulting in a camel-back structure. Such band structures have been deduced from earlier transport and tunneling experiments from single $HgTe/Hg_{1-x}Cd_xTe$ [4] and GaAs/AlAs quantum wells [5]. The resonant magnetotunneling studies of a single GaAs quantum well are particularly relevant [5]. By varying both an applied voltage and a high magnetic field, the dispersion of the states in the GaAs quantum well could be indirectly measured, leading to the assertion that the GaAs quantum well exhibited an inverted band structure [5]. Clearly, the most direct method to measure the dispersion of a band is via ARPES, and our data provide definite proof that there is significant heavy-hole and light-hole mixing in the accumulation layer of InN. An inverted band structure has also been measured in an ARPES study of an *extrinsic* quantum well formed by an indium overlayer on *p*-type Si(111) [6].

The hypothesis that the accumulation layer potential is causing this inverted band structure could be tested by measuring the valence band dispersion in the absence of the sub-bands (*i.e.*, outside the potential well). Ideally one could measure ARPES from heavily doped *n*-type InN ($n > 4 \times 10^{21}\,\mathrm{cm}^{-3}$), where little or no band bending would be required to achieve charge neutrality at the near surface [11,12] and consequently removing the potential well. Such a doping-induced change in the space-charge profile, from electron accumulation to electron depletion, has been observed for InAs using high-resolution electron energy loss spectroscopy [13]. However, given the prerequisite of high quality, well-ordered surfaces for ARPES measurements combined with the lack of such quality material with very high doping, such an experiment is not yet possible. As an alternative, we have used ARPES to measure the valence band dispersion in the ΓA direction (normal to the surface), and along a line in *k*-space parallel to the ΓA direction, outside the region where the quantum well states are observed.

Figure 3 presents two series of ARPES spectra where the incident photon energy is swept from 57 eV to 83 eV. In fig. 3(a) the spectra are recorded in normal emission with the sample normal set parallel to the spectrometer lens axis ($k_{\parallel} = 0\,\mathrm{Å}^{-1}$); these spectra correspond to emission from states along the ΓA direction in the bulk Brillouin zone. In fig. 3(b), the sample normal is set 3° off-normal with respect to the spectrometer axis, in the ΓΣM-plane. Since we record full photocurrent intensity maps as in fig. 1(a) at each photon energy, we are able to extract the EDCs shown in fig. 3(b) that correspond to emission from states that lie along a line in the Brillouin zone parallel to the ΓA direction. The 3° angle and orientation of the sample are chosen to probe a line parallel to ΓA, but not through the bulk zone center. The probed states lie at a constant offset of $k_{\parallel} = 0.21\,\mathrm{Å}^{-1}$ along the ΓM direction. Also plotted in fig. 3(c) is the predicted bulk band structure along the ΓA direction, calculated using hybrid density functional theory within the GW framework [10,14]. There is good agreement between the evolution of spectral features in fig. 3(b) and the predicted valence band dispersion along the ΓA direction. At zone center, theory predicts three peaks in the EDCs, at 0 eV, 1 eV, and 6 eV below the VBM. For EDCs excited with photon energies near 71 eV, fig. 3(b) reveals two clear features at the top of the valence band with a 1 eV separation, and a less well-defined shoulder 5 eV below these, consistent with the calculation for states at Γ. As the photon energy is increased or decreased the spectra in fig. 3(b) reflect the states predicted at the A-point. The calculation predicts two states at the A-point, with a separation of approximately 3 eV. Although exhibiting less well-defined spectral features than for the spectra recorded at 71–73 eV, examination of the spectrum recorded at 57 eV shows regions of high intensity centered near 3 and 6 eV below E_{F}, consistent with excitation of states near the A-point. The fact that the spectra in fig. 3(b) recorded with photon energies near 71–73 eV reflect states near Γ, implies that spectra excited with photon energies near 71–73 eV in *normal emission* reflect states not just at the two-dimensional surface zone center $\bar{\Gamma}$, but also at the three-dimensional bulk zone center, within the accumulation layer.

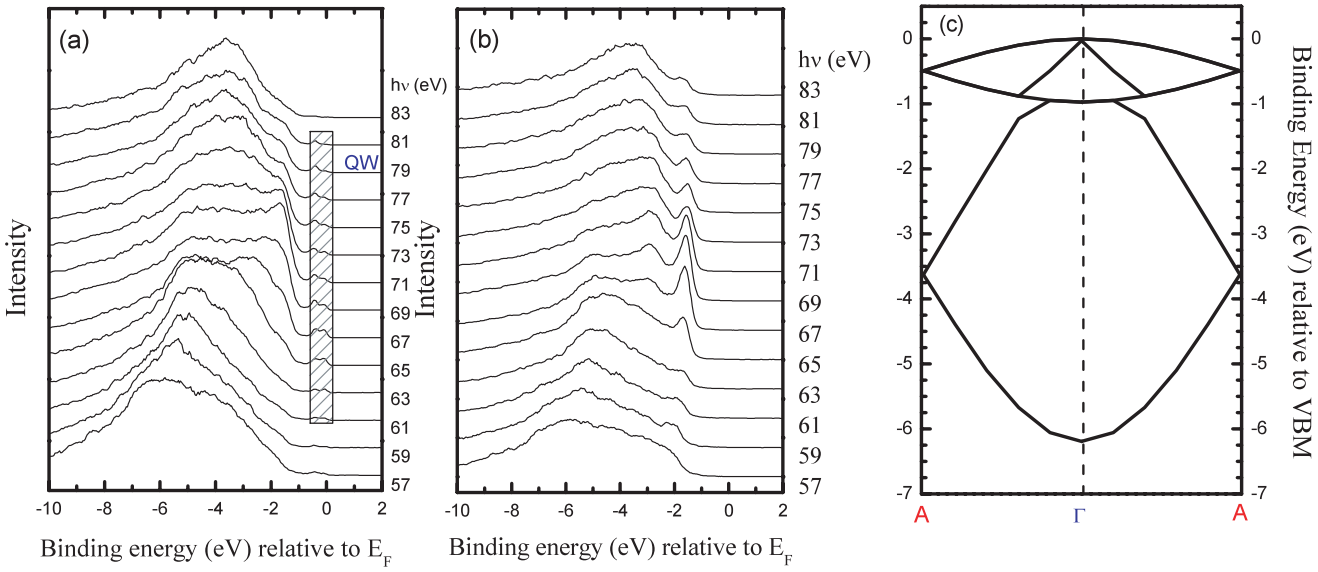

Fig. 3: A series of ARPES spectra from InN corresponding to emission from states: (a) along the ΓA direction in the bulk Brillouin zone, and (b) along a line in the zone parallel to the ΓA direction, at a constant offset of $k_{\|} = 0.21\,\text{Å}^{-1}$ along the ΓM direction, see text. (c) The corresponding calculated band structure along the ΓΔA direction of the bulk Brillouin zone (from refs. [10,14]).

While the spectra in fig. 3(b) agree in broad terms with the calculation for states along ΓA, those in fig. 3(a) clearly do not. First, note that the quantum well states are clearly visible in fig. 3(a) in the incident photon energy range 61–81 eV, but absent for this range in fig. 3(b); these states are also absent in the calculation. Conversely, the intense heavy-hole peaks clearly observed in fig. 3(b) at $\sim 1.5\,\text{eV}$ below E_F at excitation energies of near 71–73 eV are now suppressed in fig. 3(a), resulting in the camel-back structure in fig. 1. Clearly the inverted band structure and minimum at the top of the valence band is a three-dimensional effect around the Γ-point for a Brillouin zone within the accumulation layer.

To conclude, we have directly measured the dispersion of the top of the valence band in InN within the intrinsic quantum well potential associated with the electron accumulation layer. We report the observation of clear intermixing between the heavy and light holes, consistent with a classic quantum-well–induced inverted band structure. Such structures have been previously observed in engineered quantum wells, but this is the first report of their observation using ARPES from an intrinsic electron accumulation layer. Gap measurements that probe only the electronic structure within this region may show a behavior quite different from that measured in the bulk.

* * *

The authors would like to thank F. Bechstedt for fruitful discussions. This work was supported in part by the DOE under RF-06-PRD-001 (subcontract from University of Nevada, Las Vegas), and by the NSF under grant No. DMR-0311792. The ALS is supported by the DOE, Materials Sciences Division under contract No. DE-AC03-76SF00098.

REFERENCES

[1] Colakerol L., Veal T. D., Jeong H. K., Plucinski L., DeMasi A., Wang S., Zhang Y., Piper L. F. J., Jefferson P. H., Fedorov A., Chen T. C., Moustakas T. D., McConville C. F. and Smith K. E., *Phys. Rev. Lett.*, **97** (2006) 237601.

[2] Mahboob I., Veal T. D., Piper L. F. J., McConville C. F., Lu H., Schaff W. J., Furthmuller J. and Bechstedt F., *Phys. Rev. B*, **69** (2004) 201307.

[3] Milun M., Pervan P. and Woodruff D. P., *Rep. Prog. Phys.*, **65** (2002) 99.

[4] Ortner K., Zhang X. C., Pfeuffer-Jeschke A., Becker C. R., Landwehr G. and Molenkamp L. W., *Phys. Rev. B*, **66** (2002).

[5] Hayden R. K., Maude D. K., Eaves L., Valadares E. C., Henini M., Sheard F. W., Hughes O. H., Portal J. C. and Cury L., *Phys. Rev. Lett.*, **66** (1991) 1749.

[6] Takeda S. N., Higashi N. and Daimon H., *Phys. Rev. Lett.*, **94** (2005) 037401.

[7] Chen T. P., Thomidis C., Abell J., Li W. and Moustakas T. D., *J. Cryst. Growth*, **288** (2006) 254.

[8] Wu J., Walukiewicz W., Yu K. M., Ager J. W., Haller E. E., Lu H., Schaff W. J., Saito Y. and Nanishi Y., *Appl. Phys. Lett.*, **80** (2002) 3967.

[9] Hofmann T., Chavdarov T., Darakchieva V., Lu H., Schaff W. J. and Schubert M., *Phys. Status Solidi C*, **3** (2006) 1854.

[10] Piper L. F. J., Colakerol L., Learmonth T., Glans P.-A., Smith K. E., Fuchs F., Furthmuller J., Bechstedt F., Chen T.-C., Moustakas T. D. and Guo J.-H., *Phys. Rev. B*, **76** (2007) 245204.
[11] Li S. X., Yu K. M., Wu J., Jones R. E., Walukiewicz W., Ager J. W. III, Shan W., Haller E. E., Lu H. and Schaff W. J., *Phys. Rev. B*, **71** (2005) 161201(R).
[12] King P. D. C., Veal T. D., Jefferson P. H., Hatfield S. A., Piper L. F. J., McConville C. F., Fuchs F., Furthmuller F., Bechstedt F., Lu H. and Schaff W. J., *Phys. Rev. B*, **77** (2008) 045316.
[13] Piper L. F. J., Veal T. D., Lowe M. J. and McConville C. F., *Phys. Rev. B*, **73** (2006) 19531.
[14] Fuchs F., Furthmuller J., Bechstedt F., Shishkin M. and Kresse G., *Phys. Rev. B*, **76** (2007) 115109.